Macromodelling and its Applications to Signal and Power Integrity

Macromodelling and its Applications to Signal and Power Integrity

Stefano Grivet-Talocia

Dept. Electronics and Telecommunications
Politecnico di Torino, Italy
stefano.grivet@polito.it

POLITECNICO DI TORINO

Outline

- Simulation of terminated interconnects
  - Frequency and time-domain analysis
- Transient analysis
  - Convolution-based approaches
  - Direct circuit simulation (when possible)
  - Black-box passive macromodeling
- Black-box passive macromodeling
  - Rational curve fitting
  - Passivity enforcement
- An application example
  - Coupled signal-power integrity analysis of a real board
- Conclusions

2

Interconnects: showcase

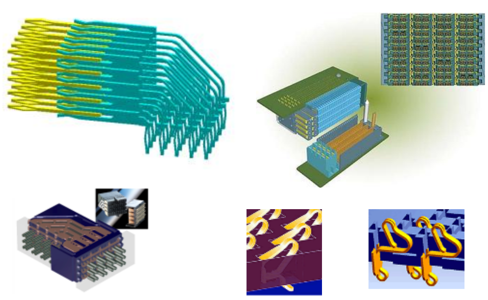

3

Interconnects: showcase

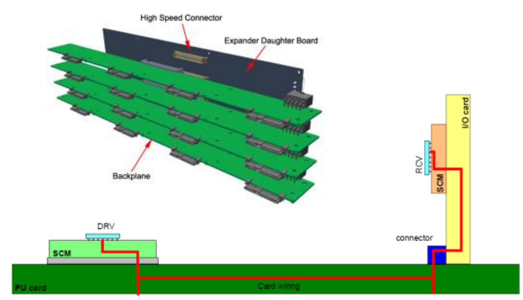

4 Courtesy D. Kaller, IBM Boeblingen, Germany

Signal Integrity

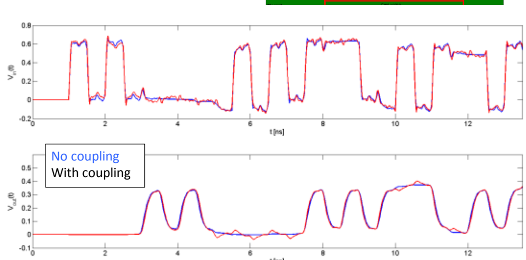

5

The objective

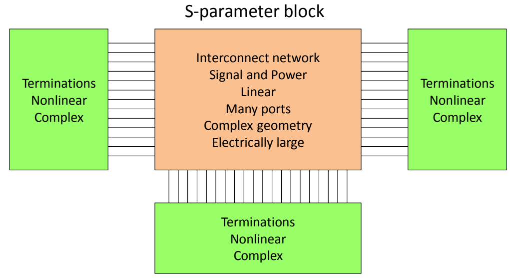

6

Nonlinear terminations

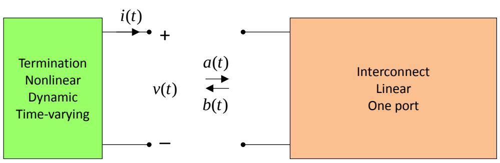

$$f\left(v, i; \frac{d}{dt}; t\right) = 0$$

$$B(j\omega_k) = S(j\omega_k)\,A(j\omega_k)$$

Inverse Fourier/Laplace transform

$$b(t) = h(t) * a(t) = \int_0^t h(t-\tau)a(\tau)d\tau$$

7

Discretizing convolution

$$b(t) = h(t) * a(t) = \int_0^t h(t-\tau)a(\tau)d\tau \qquad b(t_k) \approx \sum_{m=0}^{k-1} a(t_m)\Delta h_\Delta(t_k - t_m)$$

Memory: Number of non-vanishing time-samples in the impulse response

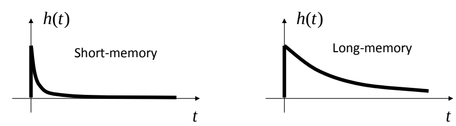

8

An example: CPU-I/O channel

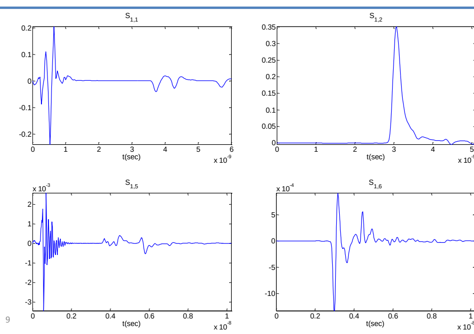

9

Direct convolution

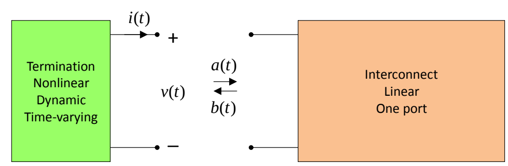

$$f\left(v, i; \frac{d}{dt}; t\right) = 0$$

$$\left.\frac{dv}{dt}\right|_{t=t_k} \approx \frac{v(t_k) - v(t_{k-1})}{\Delta}$$

$$b(t_k) \approx \sum_{m=0}^{k-1} a(t_m)\Delta h_\Delta(t_k - t_m)$$

(e.g., backward Euler)

10

Direct convolution

$$F_k\big(v(t_k), i(t_k), v(t_{k-1}), i(t_{k-1})\big) = 0$$

Need nonlinear solver

$$b(t_k) \approx \sum_{m=0}^{k-1} a(t_m)\Delta h_\Delta(t_k - t_m)$$

Use many past samples

$$a(t_k) = \frac{1}{2}\left(Z_R^{-1/2} v(t_k) + Z_R^{1/2}\, i(t_k)\right)$$

$$b(t_k) = \frac{1}{2}\left(Z_R^{-1/2} v(t_k) - Z_R^{1/2}\, i(t_k)\right)$$

May be very slow due to long memory in convolution

Very robust (when a good impulse response is available…)

11

Direct circuit simulation

If a circuit description of the interconnect is available…

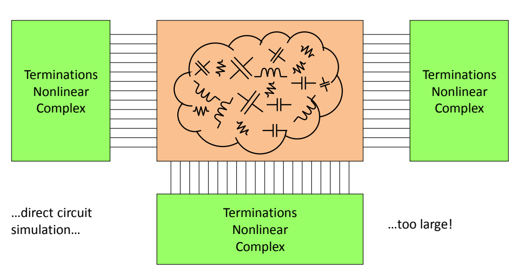

…direct circuit simulation…

…too large!

12

Model Order Reduction

Spatial discretization of Maxwell equations
(FDTD, FEM, MoM, PEEC, …)

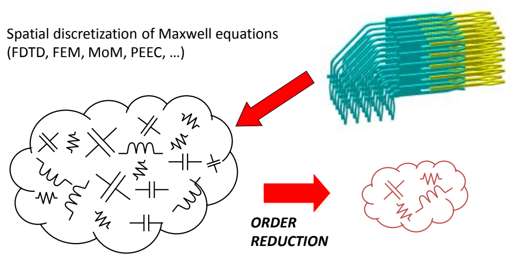

$\mathbf{S}(s) \approx \mathbf{S}_q(s)$

13

Black-Box Macromodeling

$$\mathbf{h}(t) = \frac{1}{2\pi}\int_{-\infty}^{+\infty} \mathbf{S}(j\omega) e^{j\omega t} d\omega$$

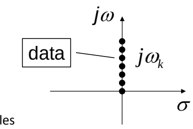

Parametric closed-form model fitting frequency samples

$$\mathbf{S}(s) \approx \sum_{n=1}^{N} \frac{\mathbf{R}_n}{s - p_n} + \mathbf{S}_\infty$$

Macromodeling via rational function fitting $s = j\omega_k$

Analytic inversion of Laplace transform

$$\mathbf{h}(t) \approx \sum_{n=1}^{N} \mathbf{R}_n \exp(p_n t) u(t) + \mathbf{S}_\infty \delta(t)$$

May be used directly in SPICE via equivalent circuit extraction

14

Rational function fitting: why?

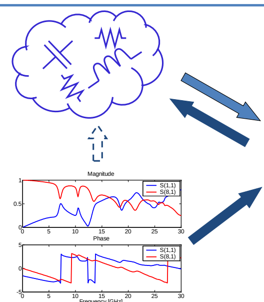

Circuit solvers understand circuits

Any lumped circuit has rational frequency responses (poles-residues, poles-zeros, ratio of polynomials)

$$\mathbf{S}(s) \approx \sum_{n=1}^{N} \frac{\mathbf{R}_n}{s - p_n} + \mathbf{S}_\infty$$

Impedance, admittance, scattering

Extraction of an equivalent circuit is an inverse problem (two-step)

15

State-space realizations

$\mathbf{a}(t)$, $\mathbf{b}(t)$

$$\begin{cases} \dot{\mathbf{x}}(t) = \mathbf{A}\,\mathbf{x}(t) + \mathbf{B}\ \mathbf{a}(t) \\ \mathbf{b}(t) = \mathbf{C}\,\mathbf{x}(t) + \mathbf{D}\ \mathbf{a}(t) \end{cases}$$

$$\mathbf{S}(s) \approx \sum_{n=1}^{N} \frac{\mathbf{R}_n}{s - p_n} + \mathbf{S}_\infty = \mathbf{D} + \mathbf{C}(s\mathbf{I} - \mathbf{A})^{-1}\mathbf{B}$$

16

Recursive convolution

$\mathbf{a}(t)$, $\mathbf{b}(t)$

Interconnect network

$$\mathbf{S}(s) = \mathbf{S}_\infty + \sum_n \frac{\mathbf{R}_n}{s - p_n}$$

$$\mathbf{h}(t) = \mathbf{S}_\infty \delta(t) + \sum_n \mathbf{R}_n e^{p_n t} u(t)$$

$$\mathbf{b}(t) = \mathbf{S}_\infty \mathbf{a}(t) + \sum_n \mathbf{R}_n \int_0^t e^{p_n(t-\tau)} \mathbf{a}(\tau) \mathrm{d}\tau = \mathbf{S}_\infty \mathbf{a}(t) + \sum_n \mathbf{R}_n \tilde{\mathbf{b}}_n(t)$$

Requires only one sample in the past!

$$\tilde{\mathbf{b}}(t_k) \approx e^{p\Delta}\tilde{\mathbf{b}}(t_{k-1}) + \frac{1 - e^{p\Delta}}{p}\mathbf{a}(t_k) \qquad t_k = t_{k-1} + \Delta$$

17

Macromodel implementations

1. Synthesize an equivalent circuit in SPICE format
   - No access to SPICE kernel
   - Must use standard circuit elements
2. Direct SPICE implementation via recursive convolution
   - Laplace element, most efficient
3. Other languages for mixed-signal analyses
   - Verilog-AMS, VHDL-AMS, …
   - Equation-based

Example: board with 13 ports

	CPU time
Standard convolution	389 seconds
Equivalent circuit	180 seconds
Recursive convolution	5.8 seconds

18

Rational curve fitting

Model: $S(s)$

3 alternative rational forms

$$S(s)=\frac{\alpha_0+\alpha_1 s+\alpha_2 s^2+\cdots+\alpha_N s^N}{\beta_0+\beta_1 s+\beta_2 s^2+\cdots+\beta_N s^N}$$

$$S(s)=\sum_{n=1}^{N}\frac{R_n}{s-p_n}+S_\infty$$

$$S(s)=S_\infty\frac{(s-z_1)(s-z_2)\cdots(s-z_N)}{(s-p_1)(s-p_2)\cdots(s-p_N)}$$

Fitting: $S(j\omega_k)\approx\ \hat{S}(j\omega_k)=\hat{S}_k \quad k=1,\cdots,K$ Input data

19

Vector Fitting

$$\hat{S}(s)\ \approx S(s)=\frac{r_0+\sum_{n=1}^{N}\frac{r_n}{s-q_n}}{c_0+\sum_{n=1}^{N}\frac{c_n}{s-q_n}}$$

Input data

"starting poles" (arbitrary, as long as distinct)

Linearized (weighted) system: multiply by the denominator

$$\left[c_0+\sum_{n=1}^{N}\frac{c_n}{s-q_n}\right]\hat{S}(s)\approx r_0+\sum_{n=1}^{N}\frac{r_n}{s-q_n} \qquad s=j\omega_k,\ k=1,\ldots,K$$

The VF "weight function" $w(s)=c_0+\sum_{n=1}^{N}\frac{c_n}{s-q_n}$

Linear Least Squares system!

20

Vector Fitting

$$w(s)=c_0+\sum_{n=1}^{N}\frac{c_n}{s-q_n}=\frac{c_0(s-q'_1)(s-q'_2)\cdots(s-q'_N)}{(s-q_1)(s-q_2)\cdots(s-q_N)}$$

"Pole relocation" process

$$\{q_n\}\rightarrow\{q'_n\}\rightarrow\cdots\rightarrow\{p_n\}$$ "true poles"

At convergence: $w(s)\rightarrow \text{constant}$

21

High-speed connector, measured

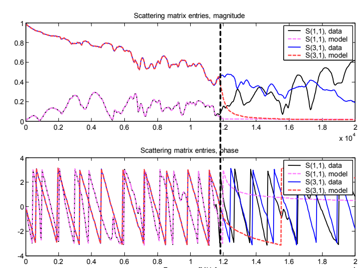

Modeled up to 12 GHz

22

Advanced VF formulations

- Time-domain Vector Fitting
  - Processes time samples instead of frequency samples
- Orthonormal Vector Fitting
  - Further improvement in matrix conditioning using orthonormal rational functions
- Z-domain (orthonormal) Vector Fitting
  - Works on discrete-time/frequency systems
- Fast Vector Fitting
  - Uses smart QR decomposition (compressions) for systems with many ports
- Eigenvalue-based Vector Fitting
  - Possibly with relative error minimization, for improved robustness
- Multivariate/Parameterized Vector Fitting
  - Allows closed-form inclusion of geometry-material parameters in the macromodel equations
- Delayed Vector Fitting
  - Uses modified basis functions for representing propagation delays in closed form
- Parallel Vector Fitting
  - For multicore hardware architectures: close to ideal speedups, almost real-time modeling

23

Passivity: why?

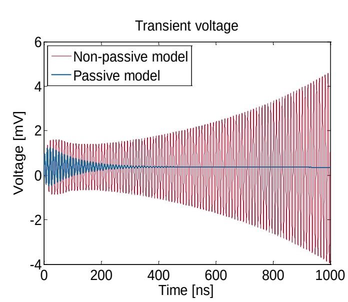

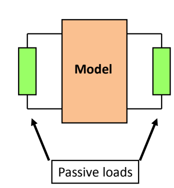

24

Passivity conditions (scattering)

1. $\mathbf{S}(-j\omega) = \mathbf{S}^{*}(j\omega)$

   Guaranteed real-valued impulse response.
   Always assumed by construction

2. $\|\mathbf{S}(j\omega)\| \le 1$ or $\max_i \sigma_i\{\mathbf{S}(j\omega)\} \le 1$

   Energy condition: structure must not amplify signals.
   Sometimes called simply "passivity" condition

3. $\mathbf{S}(j\omega)$ is causal

   No anticipatory behavior in time-domain.
   Note: causality is a prerequisite for passivity!
   Guaranteed if macromodel is stable.

25

Passivity constraints (scattering)

$\mathbf{S}(s)$ is passive $\Leftrightarrow$ {singular values of $\mathbf{S}(j\omega)$} $\le 1, \forall\omega$

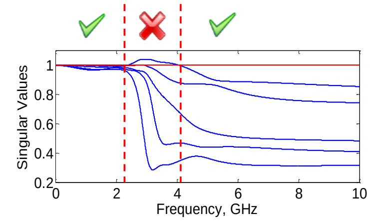

26

Passivity violations: why?

- Data from measurement
  - Improper calibration and de-embedding, human mistakes
  - Measurement noise
- Data from simulation
  - Poor meshing
  - Inaccurate solver
  - Bad models or assumptions on material properties
  - Poor data post-processing algorithms
  - Putting together results from two solvers
- Macromodel
  - Approximation errors in Vector Fitting
  - May be critical out-of-band, where no data sample is available

27

Passivity enforcement

- Generate a new passive macromodel
- Apply small correction to preserve accuracy
  - original dataset should be passive
  - original macromodel should be accurate
  - (usually) preserve poles

$$\begin{cases} \dot{\mathbf{x}} = \mathbf{A}\,\mathbf{x} + \mathbf{B}\,\mathbf{a} \\ \mathbf{b} = \mathbf{C}\,\mathbf{x} + \mathbf{D}\,\mathbf{a} \end{cases} \Rightarrow \begin{cases} \dot{\mathbf{x}} = \mathbf{A}\,\mathbf{x} + \mathbf{B}\,\mathbf{a} \\ \mathbf{b} = (\mathbf{C} + \Delta\mathbf{C})\,\mathbf{x} + \mathbf{D}\,\mathbf{a} \end{cases}$$

$$\Delta\mathbf{S} = \Delta\mathbf{C}(s\mathbf{I} - \mathbf{A})^{-1}\mathbf{B}$$

28

Model Perturbation

Singular values of S

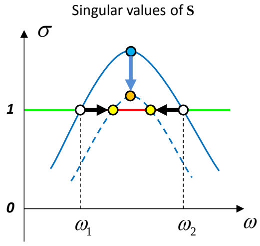

$$\begin{cases} \min \|\mathbf{w}\|_2 \\ \mathbf{Q}\,\mathbf{w} = \mathbf{y} \\ \mathbf{R}\mathbf{w} \le \mathbf{b} \end{cases}$$

accuracy

passivity

- Few and simple constraints
- Convex: robust solution

29

A case study: coupled Signal/Power Integrity

This case study courtesy of
- Georgia Institute of Technology, Atlanta GA, USA
- E-System Design, Inc.
  - Provided field solver Sphinx
- Politecnico di Torino
- IdemWorks s.r.l.
  - Provided passive macromodeling tool IdEM

E-System Design www.e-systemdesign.com
IdemWorks www.idemworks.com

30

Board cross-section

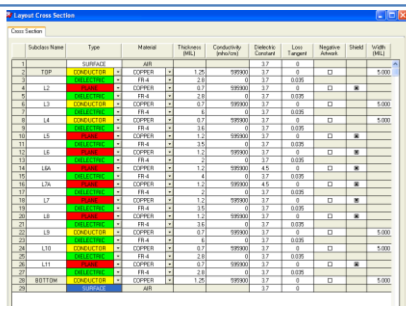
Layout Cross Section

Cross Section

	Subclass Name	Type	Material	Thickness (MIL)	Conductivity (mho/cm)	Dielectric Constant	Loss Tangent	Negative Artwork	Shield	Width (MIL)
1		SURFACE	AIR			3.7	0			
2	TOP	CONDUCTOR	COPPER	1.25	595900	3.7	0	☐		5.000
3		DIELECTRIC	FR-4	2.8	0	3.7	0.035			
4	L2	PLANE	COPPER	0.7	595900	3.7	0	☐	☒	
5		DIELECTRIC	FR-4	2.8	0	3.7	0.035			
6	L3	CONDUCTOR	COPPER	0.7	595900	3.7	0	☐		5.000
7		DIELECTRIC	FR-4	6	0	3.7	0.035			
8	L4	CONDUCTOR	COPPER	0.7	595900	3.7	0	☐		5.000
9		DIELECTRIC	FR-4	3.6	0	3.7	0.035			
10	L5	PLANE	COPPER	1.2	595900	3.7	0	☐	☒	
11		DIELECTRIC	FR-4	3.5	0	3.7	0.035			
12	L6	PLANE	COPPER	1.2	595900	3.7	0	☐	☒	
13		DIELECTRIC	FR-4	2	0	3.7	0.035			
14	L6A	PLANE	COPPER	1.2	595900	4.5	0	☐	☒	
15		DIELECTRIC	FR-4	4	0	3.7	0.035			
16	L7A	PLANE	COPPER	1.2	595900	4.5	0	☐	☒	
17		DIELECTRIC	FR-4	2	0	3.7	0.035			
18	L7	PLANE	COPPER	1.2	595900	3.7	0	☐	☒	
19		DIELECTRIC	FR-4	3.5	0	3.7	0.035			
20	L8	PLANE	COPPER	1.2	595900	3.7	0	☐	☒	
21		DIELECTRIC	FR-4	3.6	0	3.7	0.035			
22	L9	CONDUCTOR	COPPER	0.7	595900	3.7	0	☐		5.000
23		DIELECTRIC	FR-4	6	0	3.7	0.035			
24	L10	CONDUCTOR	COPPER	0.7	595900	3.7	0	☐		5.000
25		DIELECTRIC	FR-4	2.8	0	3.7	0.035			
26	L11	PLANE	COPPER	0.7	595900	3.7	0	☐	☒	
27		DIELECTRIC	FR-4	2.8	0	3.7	0.035			
28	BOTTOM	CONDUCTOR	COPPER	1.25	595900	3.7	0	☐		5.000
29		SURFACE	AIR			3.7	0			

Layers L2 and L3

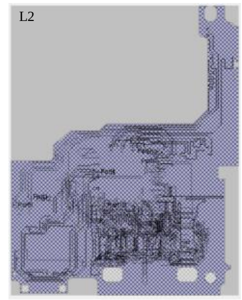

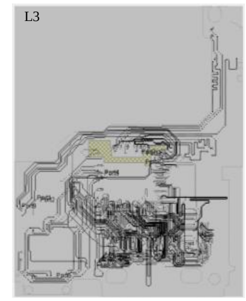

Port locations
L3 (Ref: L2) ports 1,7; 2,3; 8,9

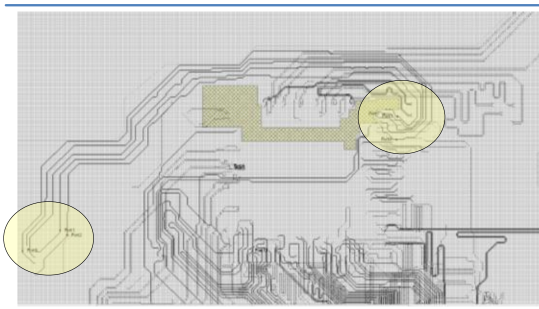

Port locations
L4 (Ref: L5) ports 10,11

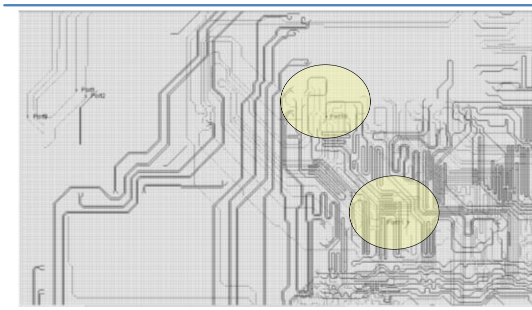

Power ports
L2 (Ref: L5) ports 12,13

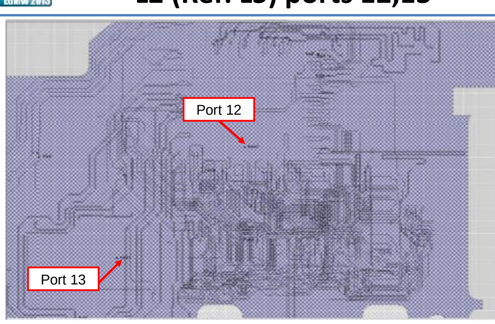

Macromodel vs S-parameters

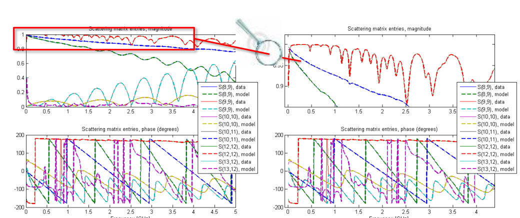

SPICE: excitation on signal lines

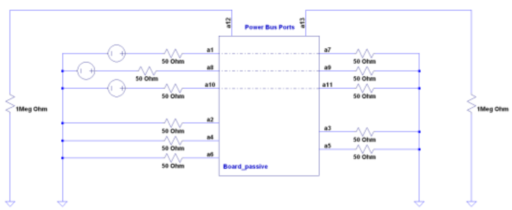

37

Response on a signal line, 1.3GHz

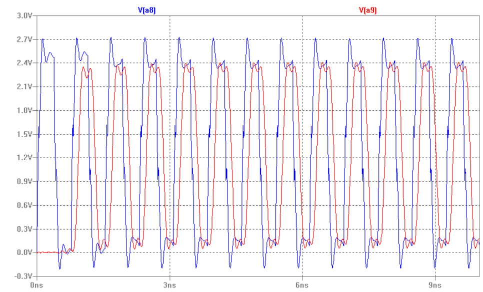

38

Coupling to power ports, 1.3GHz

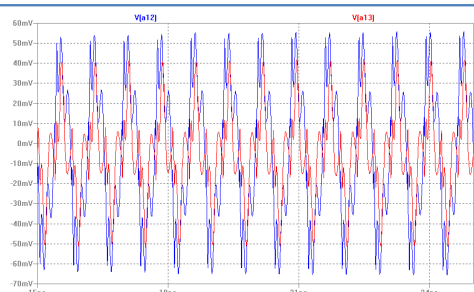

39

Xtalk and substrate coupling, 1.3GHz

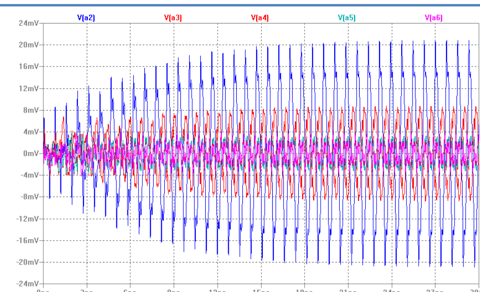

40

SPICE: excitation on PDN (core switching)

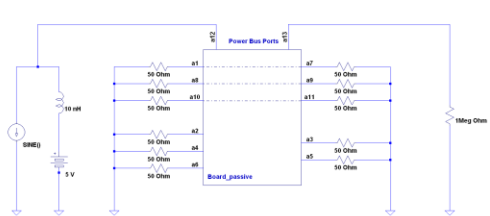

41

Decoupling capacitors

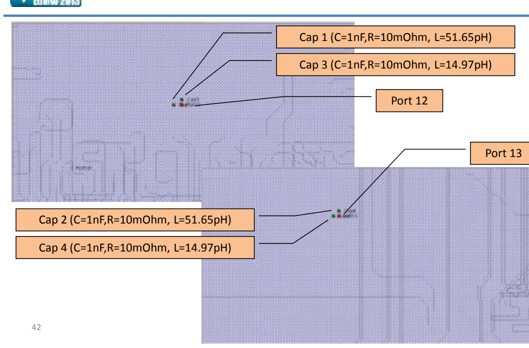

42

PDN response

Port 13: With and Without Caps

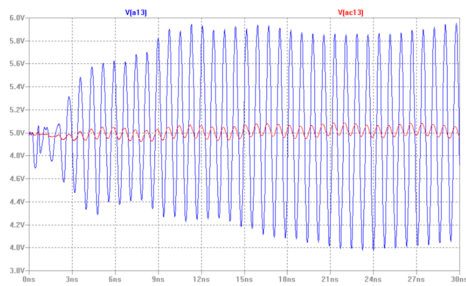

43

Eye diagram simulation: setup

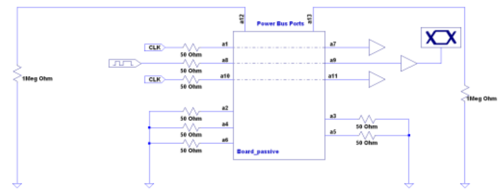

44

Eye diagram results, 2.6 Gb/s

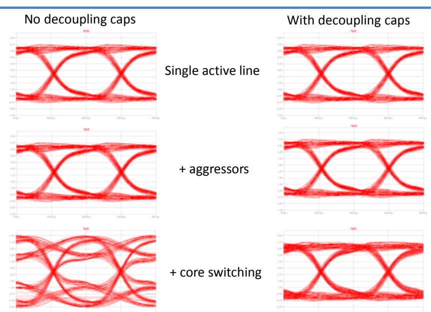

45

„Signal Integrity Summary“

- **Application:**
  - **Fast numerical assessment of Signal and Power Integrity problems during early design stages**
- **Problems:**
  - **Mixing time-domain circuit-level models (NL) with frequency-domain description of interconnect networks, complexity, efficiency**
- **Solution:**
  - **Rational black-box macromodeling + smart implementation**
  - **Key enabling factors for fast system-level simulation, design optimization, what-if analyses**

October 7, 2013 Christian Schuster 46